

## ONLINE PROCESS CONTROL FOR CENTRIFUGAL MICROMIXING

Stefan Haerberle, Roland Zengerle, and Jens Ducreé

IMTEK - University of Freiburg, Laboratory for MEMS Applications,  
Georges-Koehler-Allee 106, D-79110 Freiburg, Germany

### ABSTRACT

This paper describes a novel hydrodynamic principle for online process control of flow rate ratios and mixing between two concurrent flows in our recently introduced centrifugal micromixer [1][2]. These flows are contacted in an asymmetric, planar Y-structure on a rotating disk and subsequently driven through a common radial mixing channel. We show that the ratio of the incoming flow rates is statically seeded by the asymmetry of the inlets. The ratio can dynamically be adjusted by the frequency of rotation to realize a feedback process control. Furthermore, a new mechanism of quasi instantaneous mixing is activated by the sense of rotation. The proposed hydrodynamic mechanism is validated by experiments and simulations.

**Keywords:** Centrifugal microfluidics, micromixing, high throughput, process control

### INTRODUCTION

Chemical micro process engineering which is also termed microreaction technology has become a swiftly emerging branch of microfluidic MEMS within the last decade [3][4][5][6][7]. The often cited benefits of a tight control of heat and mass transport are rooted in increased surface to volume ratios in the micro domain. Since fast and homogeneous mixing is a pivotal constituent in chemical process engineering, a lot of different mixing concepts have been presented in the past [8][9]. Most of them utilize high aspect ratio microfluidic structures for the multilamination of pressure driven laminar flows. This however makes the fabrication of these mixing devices both complex and expensive, and it restricts the maximum throughput of a single mixing unit.

We here pursue an alternative, centrifuge-based approach to propel the flow through microfluidic channels. Such centrifugal microfluidic systems have so far primarily been employed for an integrated processing of small liquid volumes in a stopped flow ("batch") operation mode in analytical applications [10][11]. We recently extended the centrifugal platform towards continuous, high-discharge reactive micromixing applications for micro process engineering [1][2]. Besides the centrifugal force, we demonstrated that the immanent Coriolis (pseudo) force induces a

transversal stirring of concurrent radial flows to remarkably enhance mixing. The scope of applications for such a centrifugal, continuous-flow micromixer can greatly be extended with the availability of a precise control of the flow rate ratio between the two liquid sub-streams. We here present a method to seed asymmetric flow rate ratios by the geometrical asymmetry of the inlet structure and, in addition, to realize an online adjustment of the flow rates as well as the course of mixing via the sense and the frequency of rotation.

### SETUP AND FLOW SCHEME

Our centrifugal micromixing platform consists of a microstructured disk featuring fluidic channels (Fig. 1) and a rotating drive unit (e.g. standard lab centrifuge). The microchannels are fabricated in a polymeric substrate using standard micro-machining technologies and sealed by a polymeric cover-foil in a thermal diffusion bonding process. The flow patterns emerging during the mixing process at high-speed rotation can be observed from a top view through the transparent lid as greyscale pictures using a stroboscopic measurement setup developed in our lab [12]. The mixing educts are continuously injected into the rotating reservoirs on top of the disk by free-jet dispensers. After the flows are

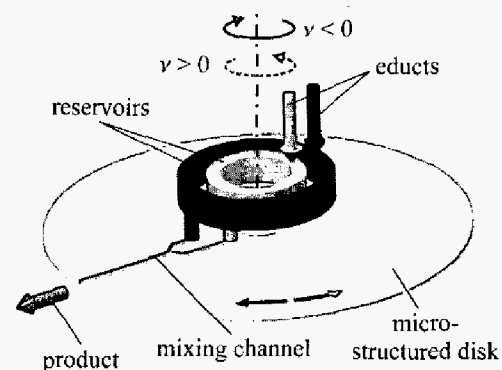


**Fig. 1.** Flow scheme of the micromixer. Two educts are injected in a contact-free fashion into receiving reservoirs on top of the microstructured disk rotating with a rotational frequency  $\nu$ . Subsequently, they are guided through the Y-shaped channel structure, and merged at a junction point. After passing the mixing channel, the mixing product is ejected through an orifice in the side-surface of the disk.

### TRANSDUCERS'05

The 13th International Conference on Solid-State Sensors, Actuators and Microsystems, Seoul, Korea, June 5-9, 2005

0-7803-8952-2/05/\$20.00 ©2005 IEEE.

contacted in a simple Y-structure and driven through the radial mixing channel, the product is ejected in a free jet out of the side-surface of the disk. This flow scheme spares the need for pressure tight fluidic micro-to-macro interfaces since the liquids are “pumped” by the centrifugal force  $F_v$  that is transmitted over the mechanical interface (disk fitting). Thus, the system can be split into a very robust and re-usable macro-device (i.e. rotational driving engine and dispensers), and the passive and possibly disposable microstructured disks.

### WORKING PRINCIPLE

Two centrifugally driven inlet flows  $\Phi_1$  and  $\Phi_2$  are joined at a clashing angle  $\alpha$  in a planar and asymmetric Y-structure (Fig. 2). The junction is located at a radial position of 3 cm followed by a 3 cm long outlet channel of cross-section  $w_{ch} \times d_{ch}$ . The asymmetry is summarized by the geometric coefficient

$$\beta = \frac{h_1 \cdot R_2}{h_2 \cdot R_1} \quad (1)$$

which depends on the heights  $h_i$  ( $i \in \{1,2\}$ ) of the two inlets and the lengths  $R_i$  of the flow resistances (cross-section:  $w_{ch} \times d_{ch}$ ). The broad upper sections (width: 1 mm, depth: 400  $\mu\text{m}$ ) are considered to have a negligible influence on the flow resistances. In our experiments, the parameters:  $h_1 = 20.5$  mm,  $h_2 = 13.5$  mm and  $R_2 = 4.5$  mm are kept constant; all other parameters of the 4 mixing structures are compiled in Table 1.

The radial flow components are chiefly influenced by the centrifugal force  $F_v \sim v^2$  (magnified insert in Fig. 2). Hence, the total discharge (outlet flow  $\Phi_1 + \Phi_2$ ) is independent of the sense of rotation, scaling with the square of the rotational frequency  $v$ . The flow rate ratio ( $\Phi_1 / \Phi_2$ ) and thus the lateral position of the mutual interface however are governed by the transversal resulting force  $F_{clash} + F_C$  within the junction. The first constituent  $F_{clash}$  accounts for the deviating hydrostatic pressure heads across the inlet channels and the so-induced difference in the kinetic energies of the two sub-streams  $\Phi_1$  and  $\Phi_2$ .  $F_{clash}$  depends on  $v$ ,  $\sin \alpha/2$ , and on  $\beta$ . The direction of the other constituent, the Coriolis force  $F_C \sim v^3$  is selected by the sign of  $v$ .  $F_C$  can either

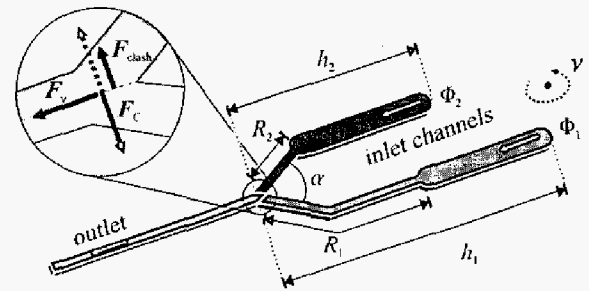


**Fig. 2.** Y-shaped asymmetric mixing structure. Two educt flows  $\Phi_1$  and  $\Phi_2$  are contacted at a clashing angle  $\alpha$ . The compound outlet flow rate  $\Phi_1 + \Phi_2$  scales with the centrifugal force  $F_v \sim v^2$ . The two transversal forces  $F_{clash}$  and  $F_C$  set the hydrodynamics within the junction, i.e. the flow ratio  $\Phi_1 / \Phi_2$  and the advection-enhanced mixing (“thumb effect”). While the direction of  $F_{clash}$  is set by the geometrical asymmetry, the direction of  $F_C$  can be set by the sense of rotation.

counteract ( $v < 0$ ) or support ( $v > 0$ )  $F_{clash}$ . The compound force  $F_{clash} + F_C$  thus acts as a frequency-adjustable setscrew to shape the contact surface within the junction towards elevated  $v$ . This, on the one hand, allows the dynamic adjustment of the flow ratio within the outlet channel. On the other hand, the transversal component of  $F_{clash} + F_C$  energizes an additional advective mixing effect right at the junction – the so-called “thumb effect” which will be explained in the following section.

### EXPERIMENTS AND SIMULATIONS

We experimentally investigate the two above described effects, i.e. the dynamic adjustment of the inlet flow ratio and the additional mixing effect at the junction point of the two inlets. For this purpose, stroboscopic gray-scale images of a given radial and azimuthal region of the spinning disk are recorded at different frequencies and senses of rotation [12].

For slow clockwise rotation e.g.  $v = -5$  Hz in Fig. 3, the asymmetry ( $\beta = 1.5$ ) pushes the interface between the black (ink-colored water) and transparent (water) phase towards the shorter inlet channel i.e. to the left channel wall. As  $v$  increases, the Coriolis force  $F_C$  counteracts  $F_{clash}$  to successively equilibrate  $\Phi_1 / \Phi_2$ . Hence, the simulated flow rate ratio approaches towards unity (from 1.38 at -5 Hz to 1.22 at -35 Hz) [13]. This frequency dependent adjustment of the ratio becomes visible in the shift of the liquid interface towards the center of the channel. However, reversing the sense of rotation  $v > 0$  (Fig. 3 at  $v = 35$  Hz and Fig. 4) results in a fundamental different hydrodynamic situation.

**Table 1.** Measured geometry of the mixing structures.

|   | $\alpha$ [°] | $w_{ch}$ [ $\mu\text{m}$ ] | $d_{ch}$ [ $\mu\text{m}$ ] | $R_1$ [mm] | $\beta$ |
|---|--------------|----------------------------|----------------------------|------------|---------|
| 1 | 63           | 260                        | 195                        | 4.5        | 1.5     |
| 2 | 63           | 400                        | 185                        | 12.5       | 0.55    |
| 3 | 31           | 393                        | 287                        | 4.5        | 1.5     |
| 4 | 126          | 360                        | 240                        | 4.5        | 1.5     |

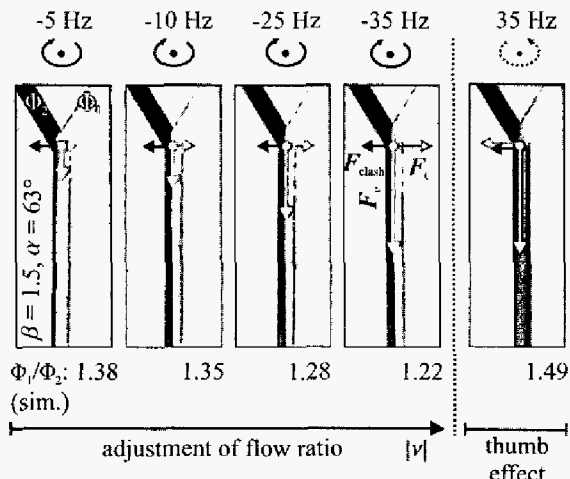


**Fig. 3.** Flow patterns at the junction for different rotational frequencies. Increasing  $|\nu|$  in clockwise, i.e. negative sense of spinning, lets the Coriolis force  $F_C$  successively neutralize  $F_{clash}$ . This shifts the liquid interface towards the center and hence  $\Phi_1 / \Phi_2$  towards unity (numerical values obtained from simulations [13]). For counter-clockwise (positive) spinning,  $F_{clash}$  and  $F_C$  are parallel, inducing an “instantaneous” advection attributed to the “thumb effect”.

The Coriolis force  $F_C$  now supports  $F_{clash}$  to suppress  $\Phi_2$ . Beyond a critical frequency  $\nu_c$ , a new type of lateral advection is observed within the junction. It is attributed to the hydrodynamic “thumb” pushed by  $F_{clash} + F_C$  against the flow  $\Phi_2$ . As the parabolic velocity profile is peaked in the center,  $\Phi_2$  is forced to escape in a tight jet along the perimeter of the “thumb” where the velocity

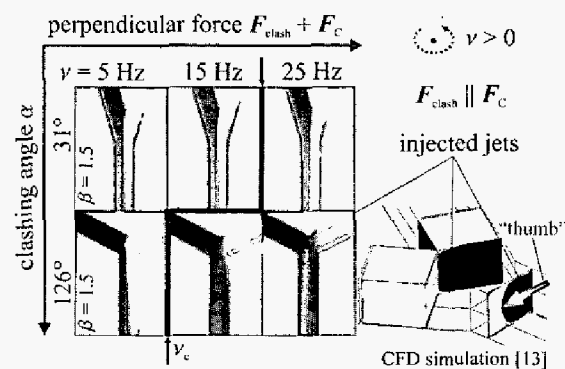


**Fig. 4.** Investigation of the “thumb effect”. For  $\nu > 0$ ,  $F_{clash}$  is parallel to  $F_C$ . The perpendicular force  $F_{clash} + F_C$  thus rapidly increases with  $\nu$  and the clashing angle  $\alpha$ . Due to its velocity-dependence,  $F_C$  is peaked in the center of the channel. A “thumb” is formed to squeeze down  $\Phi_2$ . Above a critical frequency  $\nu_c$ , this “thumb” constrains  $\Phi_2$  to inject a tight jet through a slit along the channel wall, thus boosting lateral advection in the intersection.

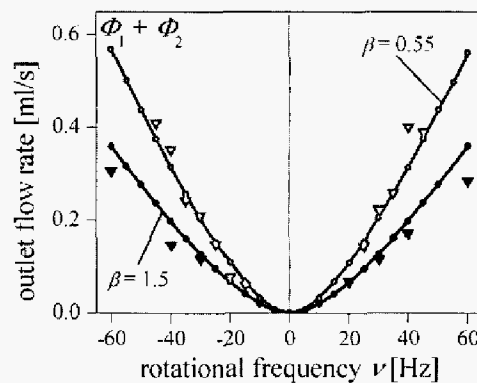


**Fig. 5.** The overall outlet flow rate  $\Phi_1 + \Phi_2$  through the radial mixing channel has been simulated ( $\blackrightarrow$ ) and measured ( $\blacktriangledown$ ) for two different asymmetric structures ( $\beta = 0.55$  and  $\beta = 1.5$ , both at  $\alpha = 63^\circ$ ). The flow rates are independent of the sense of rotation and scale with the square of the frequency  $\nu$ . This is in good agreement to the theory of centrifugal driven flows.

dependent counterforce  $F_C$  is minimum (Fig. 4, right). This initial jet injection appreciably accelerates mixing prior to the recently described, continuous “stirring” along the outlet [2]. The critical frequency  $\nu_c$  above which this effect can be observed depends on the clashing angle  $\alpha$  of the two inlet channels. With growing angles  $\alpha$ , the flow vectors of the two sub-streams are increasingly directed against each other, leading to higher clashing forces  $F_{clash}$ . Consequently, the thumb effect already occurs at reduced rotational frequencies. Furthermore, towards wider clashing angles, the fluid sub-streams have to pass through smaller bending radii, thus causing an additional centrifugal force at the junction. This centrifugal force is more pronounced within the faster sub-stream and thus possibly likewise assisting the thumb effect.

The flow rates  $\Phi_1$  and  $\Phi_2$ , respectively, have been measured by observing the change in time of the liquid level in the receiving reservoirs during rotation. According to the previous arguments, the overall outflow rate  $\Phi_1 + \Phi_2$  constitutes a nearly symmetric function in  $F_\nu \sim \nu^2$  (Fig. 5). In addition, this discharge rate is influenced by the length ( $R_i$ ) and the cross-section ( $w_{ch} \times d_{ch}$ ) of the inlets, governing the overall resistance of the Y-structure. Extraordinarily high volume throughputs are obtained towards higher frequencies of rotation (e.g.  $\sim 0.6$  ml / s at 60 Hz). This demonstrates the amenability of the centrifugal micromixing platform for production-scale applications as a generic “spoke wheel” parallelization scheme of the channels would allow to multiply the throughput per channel by a factor of about 100 per disk.

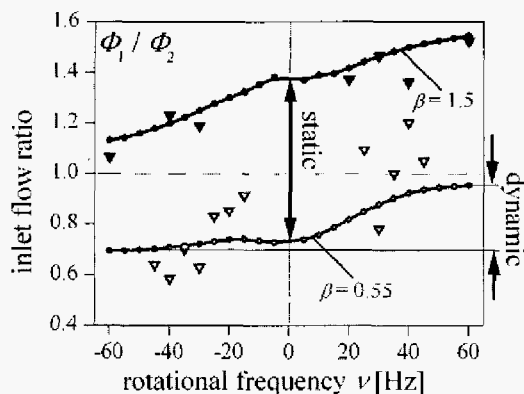


**Fig. 6.** The ratio of the inlet flow rates  $\Phi_1 / \Phi_2$  is adjusted between 0.7 and 1.4 ( $|\nu| < 60$  Hz) by the static geometrical coefficient  $\beta$  (both at  $\alpha = 63^\circ$ ). It can be tuned dynamically via the frequency of rotation  $\nu$ . The experiments ( $\blacktriangledown$ ) become increasingly unstable and deviate from the simulations ( $\rightarrow$ ) towards small  $\beta < 1$ .

The geometric coefficient  $\beta$  sets the base value for the inlet flow ratio  $\Phi_1 / \Phi_2$  (Fig. 6) at the “virtual-zero” frequency of rotation (i.e. 0 Hz). That is because all the effects that cause a shift of the liquid interface at the junction depend on the sense and the frequency of rotation and are consequently switched-off at this “virtual” situation. However, this static burned-in flow rate ratio can dynamically be adjusted by the frequency and the sense of rotation allowing an online control of mixing during the continuous process.

## SUMMARY AND CONCLUSION

We have investigated a novel method for passive and active control of flow rates, flow rate ratios and mixing in centrifugal microreaction technology. The method is of paramount interest for typical process conditions, e.g. in presence of non-uniform viscosities and educt flow rates. The option for an online adjustment with an optical feedback system also facilitates the compensation of real-world artifacts, e.g. the evolution of plaque on the channel walls.

We plan to extend our micromixing platform by additional features like temperature control towards intermediate scale chemical process engineering.

## ACKNOWLEDGEMENTS

The authors are grateful to the financial support by the “Landesstiftung Baden-Württemberg” and enjoyed an excellent cooperation with HSG-IMIT and the group of Willi Bannwarth at the University of Freiburg.

## REFERENCES

- [1] J. Ducreé, T. Brenner, T. Glatzel and R. Zengerle, “A Coriolis-Based Split-and-Recombine Laminator for Ultrafast Mixing on Rotating Disks,” *Proceedings of  $\mu$ TAS 2003*, eds. M. A. Northrup, K. F. Jensen, D. J. Harrison, 603-606 (2003).
- [2] J. Ducreé, H-P. Schlosser, T. Glatzel, S. Haeberle, M. Grumann, T. Brenner, R. Zengerle, “Centrifugal Platform for High-Throughput Reactive Micromixing,” *Proceedings of  $\mu$ TAS 2004*, eds. T. Laurell, J. Nilsson, K. Jensen, D. J. Harrison, J. P. Kutter, 554-556 (2004).
- [3] W. Ehrfeld, K. Golbig, V. Hessel, H. Löwe, and T. Richter, “Characterization of Mixing in Micromixers by a Test Reaction: Single Mixing Units and Mixer Arrays,” *Ind. Eng. Chem. Res.*, **38** (3), 1075-1082 (1999).
- [4] F. G. Bessoth, A. J. deMello and A. Manz, “Microstructure for efficient continuous flow mixing,” *Anal. Commun.*, **36** (6), 213-215 (1999).
- [5] K. F. Jensen, “Microreaction engineering – is small better?,” *Chem. Eng. Sci.*, **56** (2), 293-303 (2001).
- [6] H. Pennemann, P. Watts, S. J. Haswell, V. Hessel, and H. Löwe, “Benchmarking of Microreactor Applications,” *Org. Proc. Res. & Dev.*, **8** (3), 422-439 (2004).
- [7] G. M. Greenway, S. J. Haswell, D. O. Morgan, V. Skelton, P. Styring, “The use of a novel microreactor for high throughput continuous flow organic synthesis,” *Sensors & Actuators B*, **63** (3), 153-158 (2000).
- [8] N-T. Nguyen and Z. Wu, “Micromixers – a review,” *J. Micromech. Microeng.*, **15**, R1-R16 (2005).
- [9] V. Hessel, S. Hardt, H. Löwe, and F. Schönfeld, “Laminar Mixing in Different Interdigital Micromixers: I. Experimental Characterization,” *AIChE Journal*, **49** (3), 566-577 (2003).
- [10] L. G. Puckett, E. Dikici, S. Lai, M. Madou, L. G. Bachas, and S. Daunert, “Investigation into the Applicability of the Centrifugal Microfluidics Platform for the Development of Protein-Ligand Binding Assays Incorporating Enhanced Green Fluorescent Protein as a Fluorescent Reporter,” *Anal. Chem.*, **76** (24), 7263-7268 (2004).
- [11] M. Gustafsson, D. Hirschberg, C. Palmberg, H. Jönvall, and T. Bergman, “Integrated Sample Preparation and MALDI Mass Spectrometry on a Microfluidic Compact Disk,” *Anal. Chem.*, **76** (2), 345-350 (2004).
- [12] M. Grumann, T. Brenner, C. Beer, R. Zengerle, and J. Ducreé, “Visualization of flow patterning in high-speed centrifugal microfluidics,” *Review of Scientific Instruments*, **76** (2), (2005).
- [13] CFD-ACE+ (ESI-Group), <http://esi-group.com>, (2005).